

Atmospheric Re-Entry

Author: John C. Adams, Jr.

There are two types of entry which control the design of manned or unmanned vehicles for hypersonic re-entry into the earth's atmosphere from space:

- Ballistic (Re-Entry Vehicles, Decoys, Mercury Capsule)
- Lifting (Maneuverable Re-Entry Vehicles, Gemini and Apollo Capsules, Space Shuttle, HL-10, ASSET, PRIME, X24-A, X24-B)

Each of these types will be illustrated below with associated system design implications. More complete information can be found in Refs. 1-6, with Ref. 1 being the primary source for trajectory flight mechanics material and Ref. 3 being the primary source for hypersonic aerodynamic/heat transfer material (like the Fay-Riddell stagnation point heat transfer rate correlation). For more detailed insight into ballistic re-entry vehicle flight dynamic (including issues such as angle-of-attack convergence, dynamic instabilities, roll dynamics, dispersion from lift nonaveraging, and control considerations) the excellent History of Key Technologies paper given in Ref. 7 is highly recommended.

Ballistic Entry

A ballistic entry is one in which the retarding force is always opposed to the line of flight, that is, a "drag" force. As shown in Appendix A, the primary design parameter for ballistic entry is the Ballistic Coefficient β

$$\beta = \frac{W}{C_D A}$$

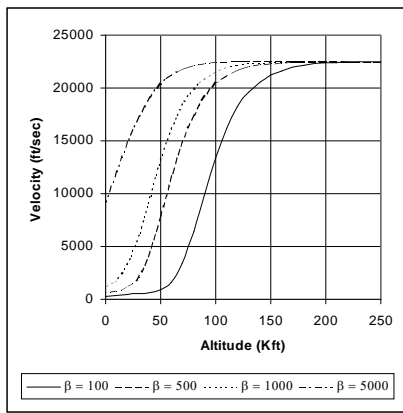
where W is the vehicle weight, C_D is the drag coefficient, and A is the reference area used in the definition of the drag coefficient. If W has units of lb_f and A has units of ft^2 , then β will have units of lb_f/ft^2 . Whenever β is used hereafter as a numerical value the units associated with it are lb_f/ft^2 . The Ballistic Coefficient β is the single most important parameter in controlling flight trajectory during entry. Heating and deceleration are less intense for a low β value (low weight and/or high drag and large frontal area) than for a high β value (high weight

and/or low drag and small frontal area) since the entry occurs high in the atmosphere where the air is less dense. Early Inter-Continental Ballistic Missiles (ICBM) with highly blunted sphere-cone-cylinder-flare geometries utilized this re-entry method. Thermal protection for these early warheads was a massive metallic heat shield, which merely provided a "heat sink" for the short heating pulse at high altitudes. It was soon discovered that delivery accuracy could be improved by increasing the values of β using slightly blunted slender sphere-cone geometries thus increasing the impact velocity so that the final descent phase was less affected by winds. Thermal protection was provided by allowing the material at the surface of the heat shield to melt or vaporize thus transferring much of the heat back into the atmosphere. This method of thermal protection is referred to as "ablation," and the material that is applied to the vehicle's outer surface is called an "ablator."

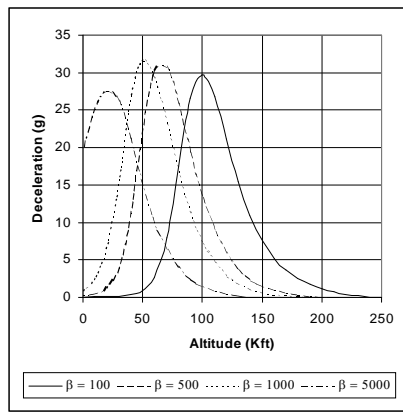
Representative ballistic earth entry trajectories are presented in Figure 1 based on application of a point mass ballistic entry computer program using the 1976 U.S. standard atmosphere model (see Appendix A). Initial entry conditions are:

Altitude = 250,000 ft
Velocity = 22,500 ft/sec
Flight Path Angle = 12 deg

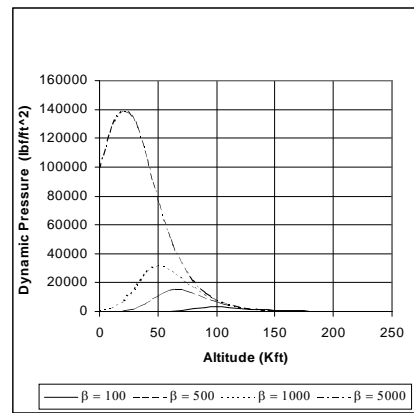
with four values of β , namely 100, 500, 1000, and 5000 (recall from the above discussion that the units on β are lb_f/ft^2). A β value between 100 and 500 is representative of the early ICBM highly blunted sphere-cone-cylinder-flare geometry, while a β value of 1000 to 5000 is representative of the slightly blunted slender sphere-cone geometry used in modern ICBM re-entry vehicles. The stagnation point heat transfer is for a sphere having a nose radius of 1.0 ft using the Fay-Riddell correlation. Note how peak deceleration, dynamic pressure, dynamic energy, stagnation point pressure, and stagnation point heat transfer are shifted to a lower altitude with increasing β . Entry times vary from slightly over three minutes for a $\beta = 100$ value to slight less than one minute for a $\beta = 5000$ value. Range distance is about 160 miles for the lowest value of β (below about 50,000 ft in altitude the vehicle has slowed to subsonic velocities and literally falls out of the sky), and increases to 190, 200, and 210 miles for the other three β values in increasing order. The flight path angle at entry controls range distance and entry times, with shallow angles increasing range distance and flight time. Further observe that modern ballistic re-entry vehicles with β values on the order of 5000 impact the earth's surface at hypersonic conditions!



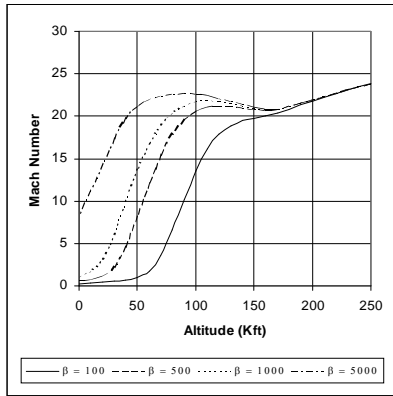
a. Velocity (ft/sec)



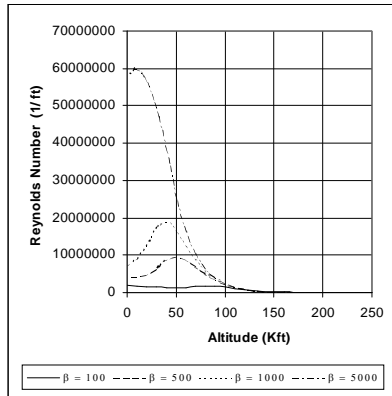
b. Deceleration (g)



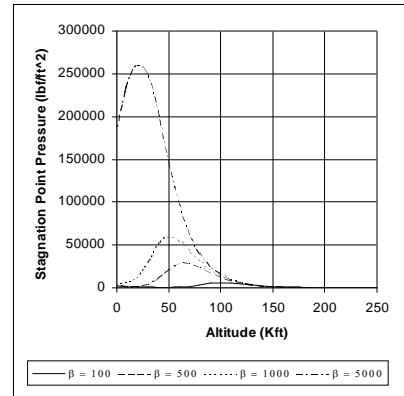
c. Dynamic Pressure (lbf/ft²)



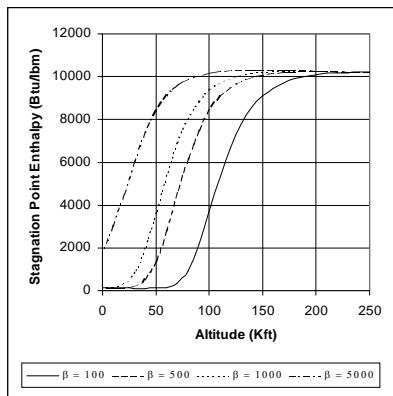
d. Mach Number



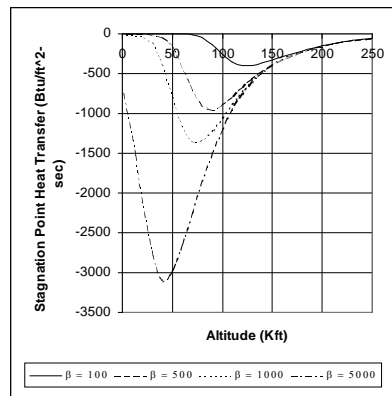
e. Reynolds Number (1/ft)



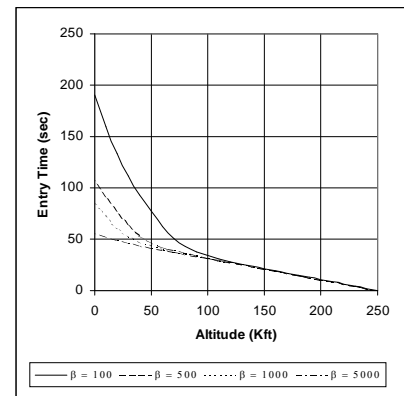
f. Stagnation Point Pressure (lbf/ft²)



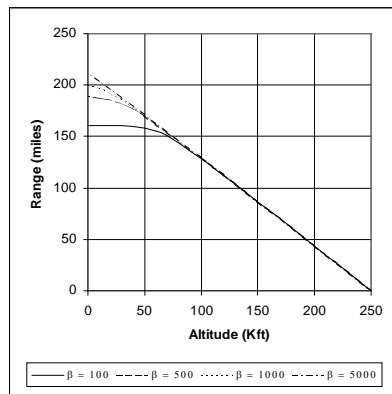
g. Stagnation Point Enthalpy (Btu/lbm)



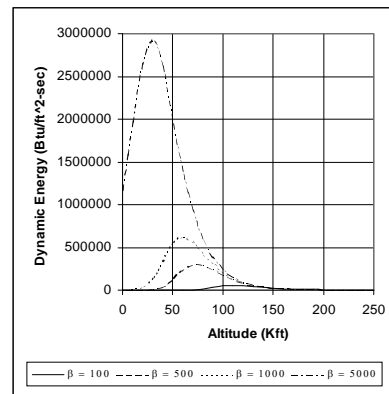
h. Stagnation Point Heat Transfer (Btu/ft²-sec)



i. Entry Time (sec)



j. Range (miles)



k. Dynamic Energy (Btu/ft²-sec)

Figure 1. Ballistic Earth Entry Trajectory.

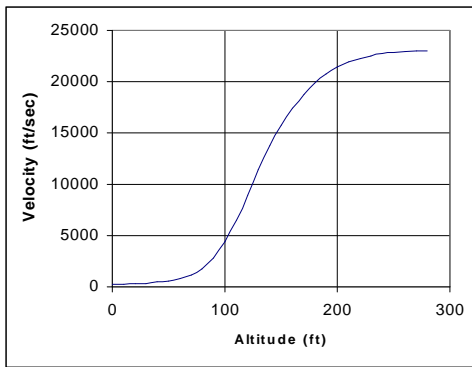
The first manned ballistic re-entry was the flight of Colonel John Glenn's "Friendship 7" Mercury capsule in February 1962. The Mercury Capsule had the following parameters:

Weight = 2662.8 lb_f
Reference Area = 30.27 ft²
Reference Length = 6.2 ft
Nose Radius (Sphere) = 1.0 ft
 $C_D = 1.60$

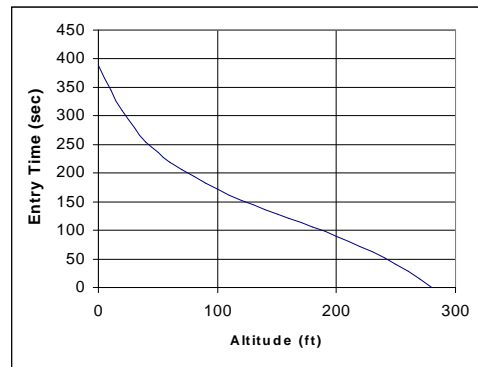
which resulted in a Ballistic Coefficient $\beta = 54.98$. Initial earth entry conditions were:

Altitude = 250,000 ft
Velocity = 23,000 ft/sec
Flight Path Angle = 1.5 deg

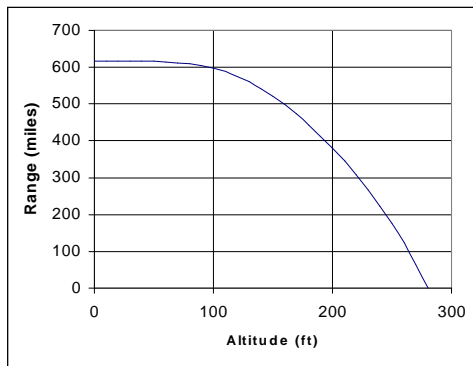
Representative "Friendship 7" Mercury capsule ballistic earth entry trajectories are presented in Figure 2 based on application of a point mass ballistic entry computer program using the 1976 U.S. standard atmosphere model (see Appendix A). The important factor to observe is that Colonel Glenn was subjected to a substantial deceleration g load (over 8) for a sustained time period of about 30 seconds. This was the impetus for the development of lifting entry for manned space flight in order to reduce sustained g loading over extended time periods.



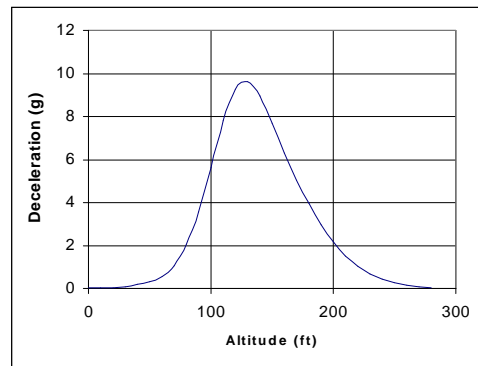
a. Velocity



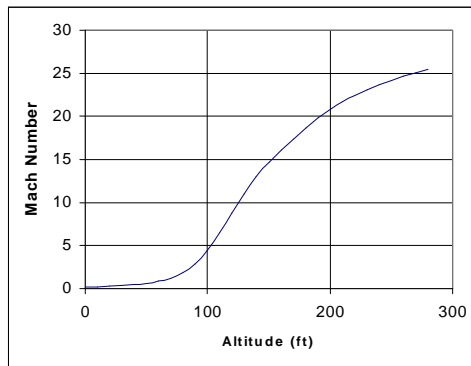
b. Entry Time (sec)



c. Range (miles)



d. Deceleration (g)



e. Mach Number

Figure 2. “Friendship 7” Mercury Capsule Earth Entry.

Lifting Entry

A lifting entry is one in which the primary force being generated is perpendicular to the flight path, that is, a "lift" force. Although drag is present throughout the entry, the resulting flight path can be adjusted continuously to change both vertical motion and flight direction while the velocity is slowing. The gliding flight of a sailplane is an example of "lifting" entry without high velocities and heating. The primary design parameter for lifting entry is the Lift to Drag Ratio, or L/D;

$$L/D = \text{Lift} / \text{Drag} = C_L / C_D$$

Low values of L/D produce moderate g loads, moderate heating levels, and low maneuverability. High values of L/D produce very low g loads, but entries are of very long duration and have continuous heating. An example is Space Shuttle re-entry at a L/D value of around unity with a total entry time of about 25 minutes. Although the peak temperatures of a lifting entry are below the peak temperature of a ballistic entry, the total heat load that must be absorbed over the duration of the entry is higher. Lateral maneuverability during entry (commonly referred to as "cross-range capability") is dramatically increased as the L/D increases.

Representative lifting earth entry trajectories for three initial values of the entry flight path angle (namely 0.1, 1.0, and 2.5 deg) are presented in Figure 3 based on application of a point mass lifting entry computer program using the 1976 U.S. standard atmosphere model (see Appendix A). Initial entry conditions are:

Altitude = 250,000 ft

Velocity = 23,000 ft/sec

with the configuration being the NASA Space Shuttle possessing the following parameters:

Weight = 200,000 lbf

Reference Area = 2690 ft²

Reference Length = 107.5 ft

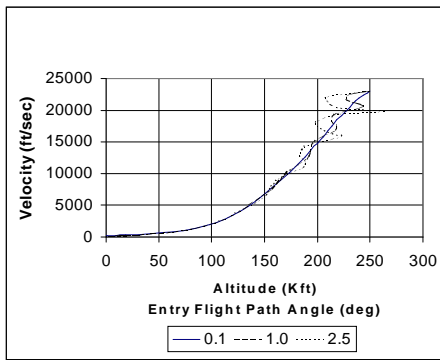
Nose Radius (Sphere) = 1.0 ft

C_D = 0.84

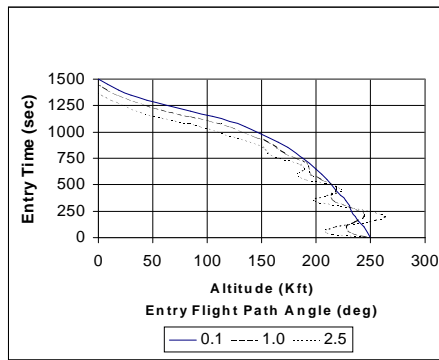
C_L = 0.84

which results in a value of the Ballistic Coefficient $\beta = 88.5$ and a Lift to Drag ratio of unity. This low value for the Ballistic Coefficient β reflects the high value

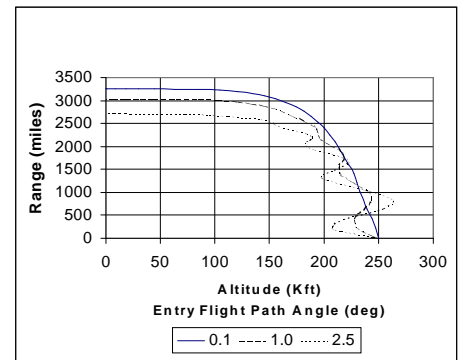
of drag coefficient (due to high angles of attack during re-entry) and large value for the reference area (the windward side planform area). The stagnation point heat transfer is for a sphere having a nose radius of 1.0 ft using the Fay-Riddell correlation. Reynolds number is based on the above specified reference length, which is basically the length of the Space Shuttle. As is obvious from the figures, entry of a lifting body with L/D ratio on the order of unity is super sensitive to the entry flight path angle. Entry with too high an entry path angle results in the vehicle flying an oscillatory trajectory at the higher altitudes, including the possibility of skipping out of the earth's atmosphere and returning to space. As is the case with ballistic entry, an increase in the entry flight path angle results in a decrease in entry time and range. The important factor to manned space flight is the significant reduction in deceleration g loads with lifting entry relative to ballistic entry. For Space Shuttle lifting entry, the astronauts will experience a deceleration g load between 0.5 and 1 as compared to the over 8 g load which Colonel John Glenn endured during his Mercury capsule ballistic re-entry. Another important factor in lifting entry is the shift of peak stagnation point heat transfer to high altitudes (over 200,000 ft) relative to ballistic entry where peak stagnation heating occurs at lower altitudes (under 100,000 to 150,000 ft). This has important consequences to the vehicle thermal protection system designer who is concerned with management of the integrated heat load over time which the vehicle structure must absorb during re-entry.



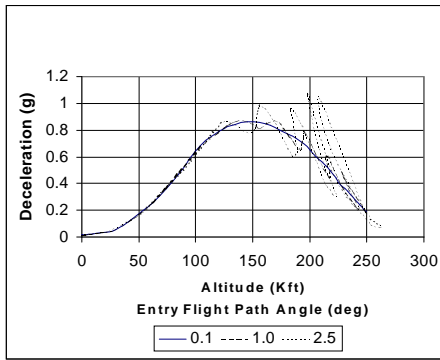
a. Velocity (ft/sec)



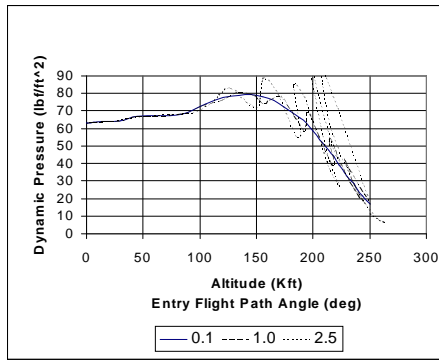
b. Entry Time (sec)



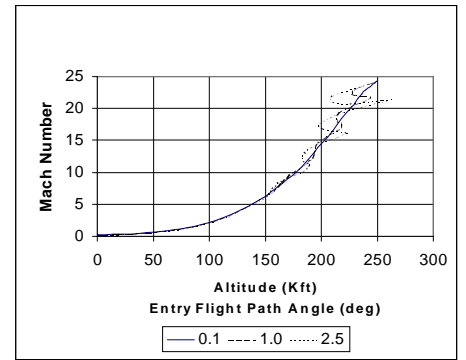
c. Range (miles)



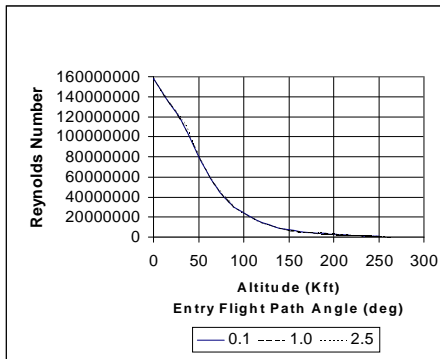
d. Deceleration (g)



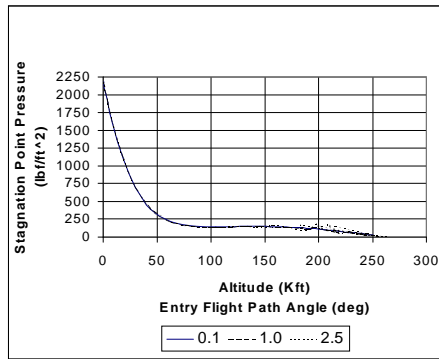
e. Dynamic Pressure (lb/ft²)



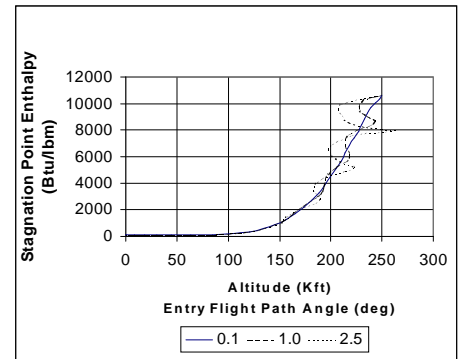
f. Mach Number



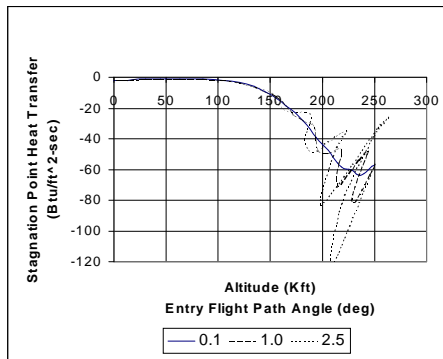
g. Reynolds Number



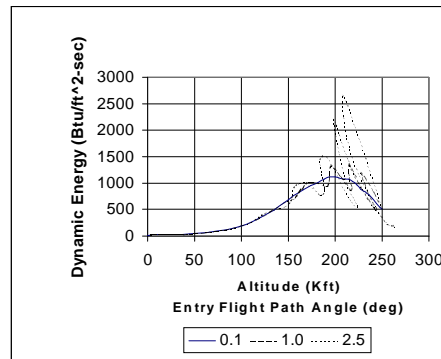
h. Stagnation Point Pressure (lb/ft²)



i. Stagnation Point Enthalpy (Btu/lbm)



j. Stagnation Point Heat Transfer (Btu/ft²-sec)



k. Dynamic Energy (Btu/ft²-sec)

Figure 3. Space Shuttle Lifting Earth Entry Trajectory.

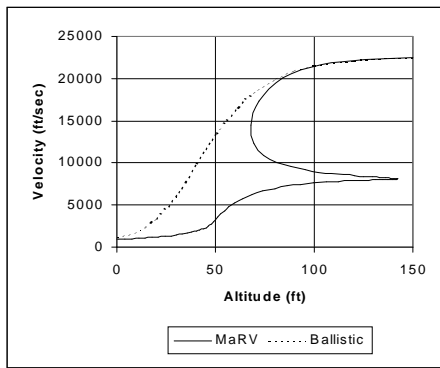
Lifting entry is a key component to flight trajectories of a Maneuverable Re-entry Vehicle (MaRV) which flies a non-ballistic trajectory to help avoid intercept by defensive systems. Shown in Figure 4 are comparisons of a representative MaRV trajectory versus a ballistic trajectory for a Ballistic Coefficient $\beta = 1000$ high performance vehicle. The initial conditions at 150,000 feet altitude correspond to ballistic entry with no lift to that point from an initial entry condition of

Altitude = 250,000 ft

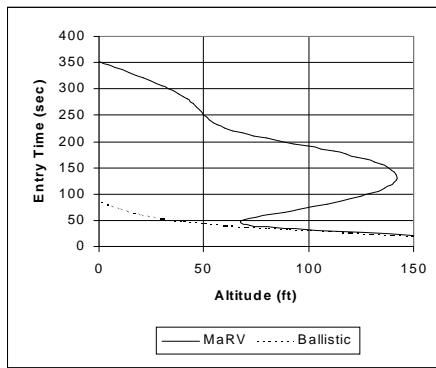
Velocity = 22,500 ft/sec

Flight Path Angle = 12 deg

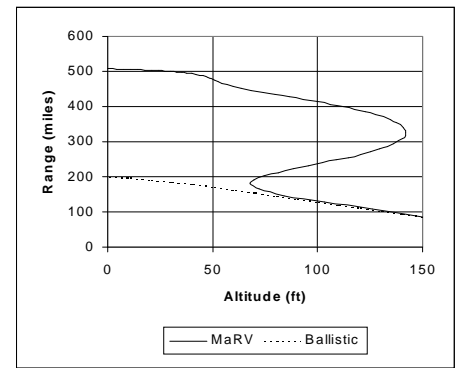
At 150,000 ft a constant $L/D = 0.5$ is applied to the MaRV trajectory for the remainder of the flight. The stagnation point heat transfer is for a sphere having a nose radius of 1.0 ft using the Fay-Riddell correlation. The MaRV continues along essentially a ballistic trajectory until about 70,000 ft, executes a pull-up (as lift becomes dominant over drag) to return to an altitude of about 140,000 ft, and then flies basically a ballistic-like trajectory to earth impact. The consequences of this maneuver is that the range is increased by a factor of about 2.5 over a pure ballistic entry; corresponding entry time is increased from about 85 seconds for pure ballistic entry to 352 seconds for lifting entry. Substantial reductions in deceleration g loads, dynamic pressure, dynamic energy, stagnation point pressure, stagnation point enthalpy, and stagnation point heat transfer result from the lifting trajectory.



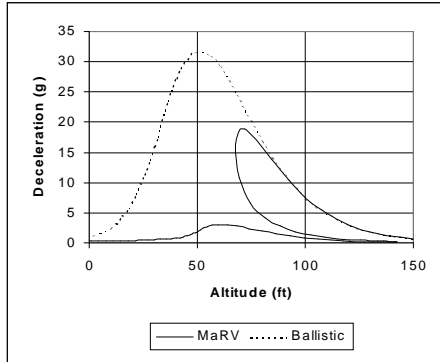
a. Velocity (ft/sec)



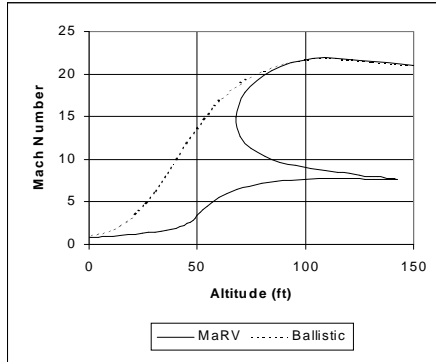
b. Entry Time (sec)



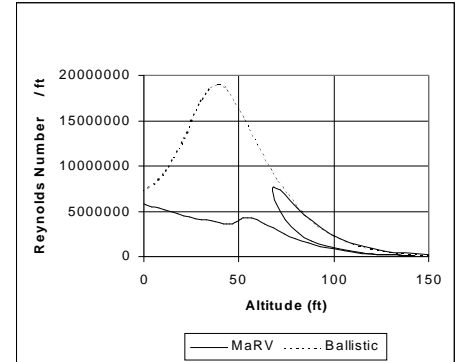
c. Range (miles)



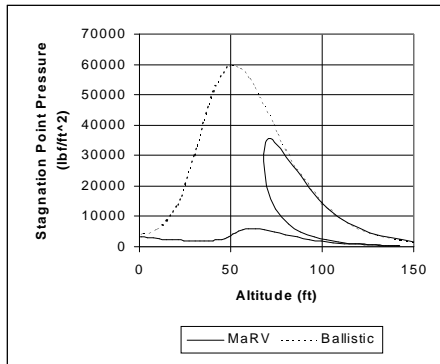
d. Deceleration (g)



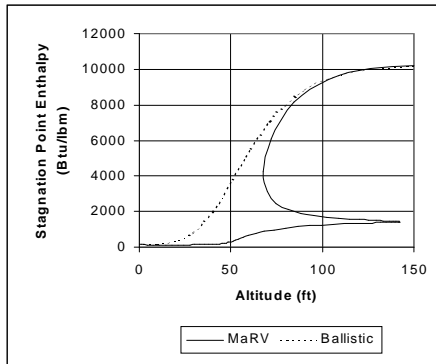
e. Mach Number



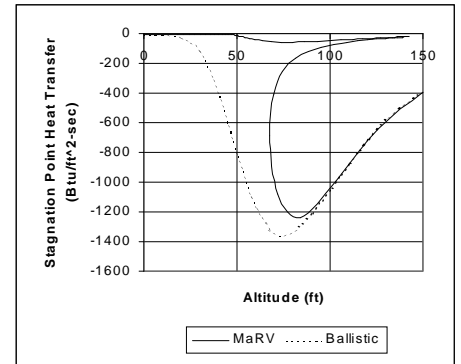
f. Reynolds Number



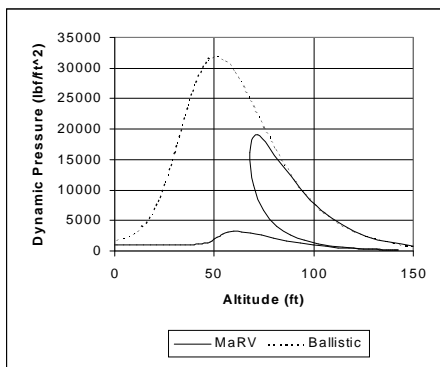
g. Stagnation Point Pressure (lb/ft^2)



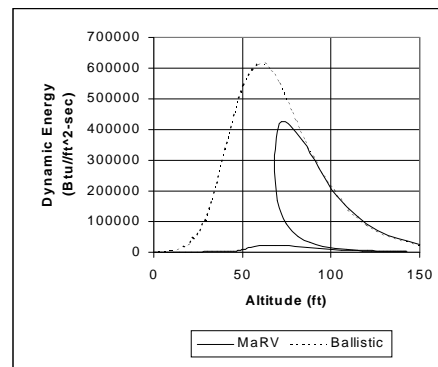
h. Stagnation Point Enthalpy (Btu/lbm)



i. Stagnation Point Heat Transfer (Btu/ft^2-sec)



j. Dynamic Pressure (lb/ft^2)



k. Dynamic Energy (Ftu/ft^2-sec)

Figure 4. MaRV vs Ballistic Trajectory.

System Implications

The above example ballistic and lifting trajectory illustrations show quite clearly that there are three primary factors available to the re-entry system designer

1. Ballistic Coefficient β
2. Lift to Drag Ratio L/D
3. Flight Path Angle at Entry

which control the flight performance of a re-entry system. Application of these factors to the design process for both ballistic and maneuverable warhead delivery systems will now be illustrated.

Modern ballistic trajectory nuclear weapon system delivery vehicles typically utilize slender sphere-cone geometries with multiple warheads on a single delivery bus (see Appendix B). For a given warhead and associated arming device, the designer selects the re-entry vehicle base diameter and vehicle length, which effectively determines the cone half-angle. The nose bluntness ratio is then selected based on drag and heat transfer considerations, with Figure 5 illustrating the effects of nose bluntness ratio on sphere-cone drag coefficient C_D for a family of sphere-cone half-angles on classical Newtonian theory.

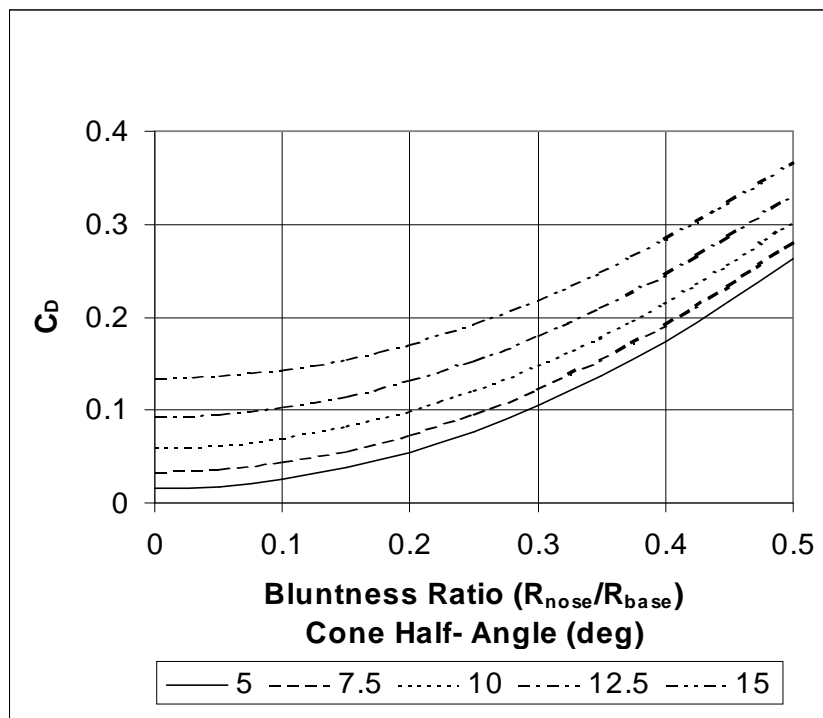


Figure 5. Classical Newtonian Drag Coefficient for a Sphere-Cone.

Vehicle weight is now fixed as the combined weight of the warhead, arming device, and re-entry vehicle. At this point the Ballistic Coefficient β is fully determined so the designer can assess ballistic trajectory performance of the design relative to mission requirements, e.g., deceleration g loads, range, and flight time. It is these mission requirements which effectively set the flight path angle at entry. Iteration of this process may be required several times before all mission requirements are fully satisfied.

A similar approach is followed for a MaRV warhead delivery system. Maneuvering is a defensive tactic that a re-entry vehicle designer uses to confound the guidance algorithms of an interceptor vehicle. There are multiple ways for the designer to provide maneuverable capability in a re-entry vehicle, such as moveable flaps which can provide one, two, or three degrees of freedom (pitch, yaw, and roll). Control can also be effected by moving a mass laterally in the vehicle to offset the vehicle's center of gravity (e.g., the Gemini capsule had a slight mass offset to provide a trim angle of attack whose direction and magnitude could be controlled by the astronaut). The resulting mass asymmetry is equivalent to an aerodynamic asymmetry. Another aerodynamic approach is jet interaction, but this appears best suited to steering out navigational errors rather than defensive maneuvering. The common element is that the additional design variable of L/D lift to drag ratio is introduced. Figure 6 illustrates the effects of nose bluntness ratio ($R_{\text{nose}}/R_{\text{base}}$) on a 10.0 deg half-angle sphere-cone lift to drag coefficient L/D based on classical Newtonian theory over an angle of attack range from zero up to the cone half-angle.

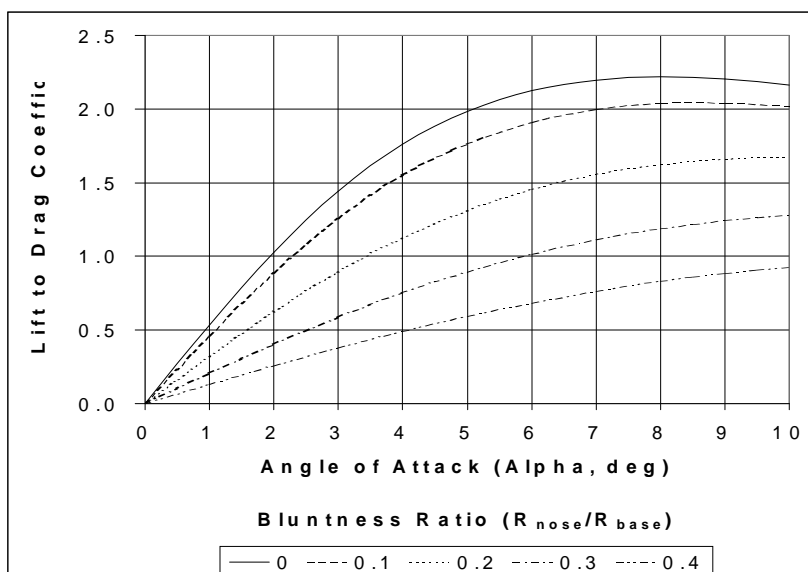


Figure 6. Classical Newtonian Lift to Drag Coefficient
For a 10.0 deg Half-Angle Sphere Cone.

High L/D requires small bluntness ratio for a sphere-cone geometry. For small bluntness ratio, a small angle of attack generates substantial lift to drag, i.e., only a little more than two degrees angle of attack is required to generate a lift to drag coefficient of unity for a 0.1 bluntness ratio. Given this sensitivity to bluntness and angle of attack, the MaRV designer must carefully incorporate lift effects into the desired maneuver control schedule. Choice of altitude at which to initiate and terminate maneuver is one of the key factors, which must be optimized based on vehicle characteristics and mission requirements.

Decoys are re-entry bodies which are intrinsically benign but which accompany warhead carrying re-entry vehicles for the purpose of confusing defense radar systems. In order for a decoy to be credible, it must present to the defense radar system a set of measurable quantities or observables, which are sufficiently close numerically to those of a hostile re-entry body to leave considerable doubt as to the threat of the vehicle. If our interest is confined to ballistic re-entry vehicles, then the key parameter, which characterizes the trajectory of the body, is the Ballistic Coefficient β . With reference to Appendix B, the weight of the warhead in a typical high performance re-entry vehicle is between 50 and 75 percent of the total vehicle weight. If the decoy has the same physical size characteristics (and thus aerodynamic drag) as the warhead carrying vehicle, then the Ballistic Coefficient β for the decoy will be between 25 and 50 percent of the warhead carrying vehicle. With reference to Figure 1, assume the warhead carrying vehicle has a β of 1000 and the decoy has a β of 500. The radar defense system will be able to detect changes in Ballistic Coefficient β below about 150,000 feet in terms of vehicle deceleration. By 100,000 ft altitude there is a factor of two difference in vehicle deceleration due to the Ballistic Coefficient β , i.e., as altitude decreases there is an increasing divergence between the measured decelerations of a decoy and the hostile re-entry vehicle. Thus the observables associated with a decoy and the warhead-carrying re-entry body become increasingly distinct with decreasing altitude. The decoy designer has many available options, such as changing the vehicle size characteristics and/or nose bluntness to alter vehicle drag, in order to achieve one paramount requirement – best match of the Ballistic Coefficient β between the warhead carrying vehicle and the decoy over the portion of the flight trajectory where the defensive system must commit to choice of target to intercept.

It is interesting to compare the differing design philosophies of the United States and Former Soviet Union ICBM delivery systems as they were developed in the 1960–1970 time frame. Shown in Figure 7 are three United States Mark-12A re-entry vehicles mounted on a delivery bus which armed a portion of the

Minuteman III ICBM Force. Each re-entry vehicle is a slender slightly-blunted sphere-cone (order of 10 degrees half-angle) with a total weight of about 800 pounds (warhead and re-entry vehicle) having a warhead yield of around 350 kilotons. Figure 8 displays a Former Soviet Union SS-6 re-entry vehicle which is a highly-blunted sphere-cone (order of 10 degrees half-angle) with a total weight of about 10,000 pounds (warhead and re-entry vehicle) having a warhead yield around 3 megatons. The United States design philosophy involved small multiple independently targeted re-entry vehicles delivered from a carrier bus with high precision accuracy while the Former Soviet Union design philosophy was a large single re-entry vehicle with a massive warhead yield to make up for any delivery inaccuracy with raw explosive power.

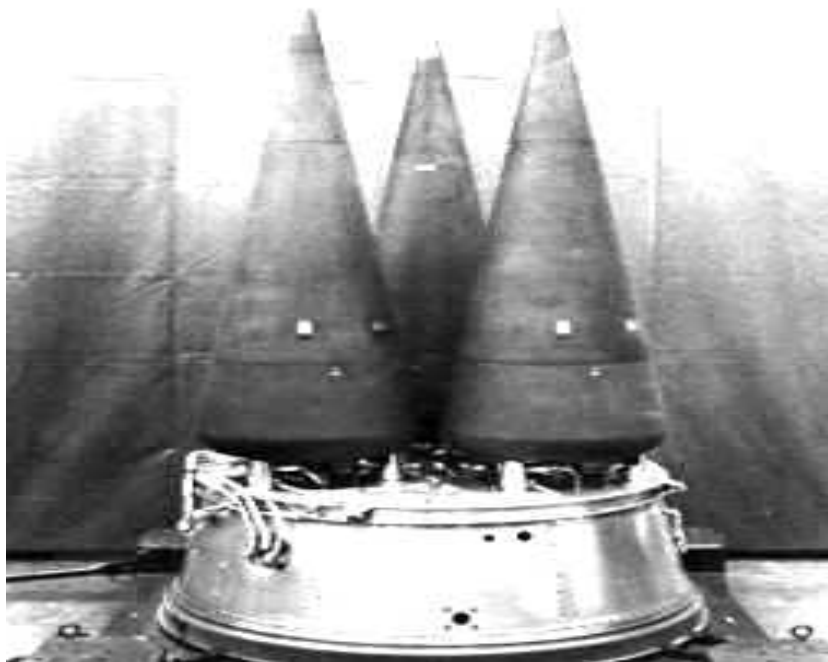


Figure 7. United States Mark-12A Re-Entry Vehicles

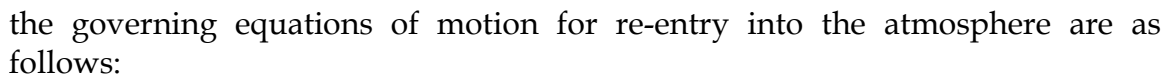


Figure 8. Former Soviet Union SS-6 Re-Entry Vehicle.

References

1. Regan, Frank J. and Anandakrishnan, Satya M. **Dynamics of Atmospheric Re-Entry**. AIAA Education Series, American Institute of Aeronautics and Astronautics, Washington, DC, 1993.
2. Regan, Frank J. **Re-Entry Vehicle Dynamics**. AIAA Education Series, American Institute of Aeronautics and Astronautics, Washington, DC, 1984.
3. Bertin, John J. **Hypersonic Aerothermodynamics**. AIAA Education Series, American Institute of Aeronautics and Astronautics, Washington, DC, 1994.
4. Hankey, Wilbur L. **Re-Entry Aerodynamics**. AIAA Education Series, American Institute of Aeronautics and Astronautics, Washington, DC, 1988.
5. Ashley, Holt. **Engineering Analysis of Flight Vehicles**. Addison-Wesley Publishing Company, Reading, MA, 1974.
6. Martin, John J. **Atmospheric Reentry, An Introduction to its Science and Engineering**. Prentice-Hall, Englewood Cliffs, NJ, 1966.
7. Platus, Daniel H. "Ballistic Re-entry Vehicle Flight Dynamics." **AIAA Journal of Guidance, Control, and Dynamics**, Vol. 5, No. 1, January-February 1982, pp. 4-16.

Following Refs. 1-6 with the assumption of point mass planar motion over a nonrotating planet per the sketch below


$$\frac{dV}{dh} = \frac{g[\frac{Q}{\beta} - \sin(\gamma)]}{V \sin(\gamma)}$$

$$\frac{d\gamma}{dh} = \frac{\cos(\gamma)[-g + \frac{V^2}{R_e + h}]}{V^2 \sin(\gamma)}$$

$$\frac{dt}{dh} = \frac{-1}{V \sin(\gamma)}$$

$$\frac{dr}{dh} = R_e \frac{\frac{d\theta}{dt}}{\frac{dh}{dt}} = \frac{-R_e \cos(\gamma)}{(R_e + h) \sin(\gamma)}$$

Lifting trajectory with time t as the variable of integration

$$\frac{dV}{dt} = g \left[\frac{-Q}{\beta} + \sin(\gamma) \right]$$

$$\frac{d\gamma}{dt} = \frac{-\frac{Qg}{\beta} \frac{L}{D} + \cos(\gamma) \left[g - \frac{V^2}{R_e + h} \right]}{V}$$

$$\frac{dh}{dt} = -V \sin(\gamma)$$

$$\frac{dr}{dt} = R_e \frac{d\theta}{dt} = \frac{R_e V \cos(\gamma)}{R_e + h}$$

where in the above equations

V = Vehicle velocity (ft/sec)

γ = Vehicle flight path angle (radians – considered positive when the velocity vector is below the local horizontal)

h = Vehicle altitude (ft) above Earth's surface

r = Vehicle flight range (ft) along Earth's surface

t = Vehicle time of flight (sec)

R_e = Radius of Earth (20,930,000 ft)

g_e = Acceleration due to gravity at Earth's surface (32.174 ft/sec²)

g = Acceleration due to gravity at altitude h (ft/sec²)

$$g = g_e \left(\frac{R_e}{R_e + h} \right)^2$$

Q = Dynamic pressure at altitude h (lb_f/ft²)

W = Vehicle weight (lb_f)

C_D = Vehicle Drag Coefficient

A = Vehicle reference area used in definition of drag coefficient (ft²)

β = Vehicle Ballistic Coefficient (lb_f/ft²)

$$\beta = \frac{W}{C_D A}$$

C_L = Vehicle lift coefficient based on same reference area used in C_D

$$\frac{L}{D} = \frac{C_L}{C_D} = \text{Vehicle Lift to Drag Ratio}$$

With reference to the above equations, note specifically that the Ballistic Coefficient β is the single controlling parameter for ballistic re-entry flight. For lifting re-entry flight, the Lift to Drag Ratio L/D joins the Ballistic Coefficient β as joint parameters. With initial entry conditions (V , γ , h , t , r) specified from mission constraints, flight motion of the vehicle through the atmosphere is solely a function of these two independent parameters. Thus they comprise the primary factors for system design considerations.

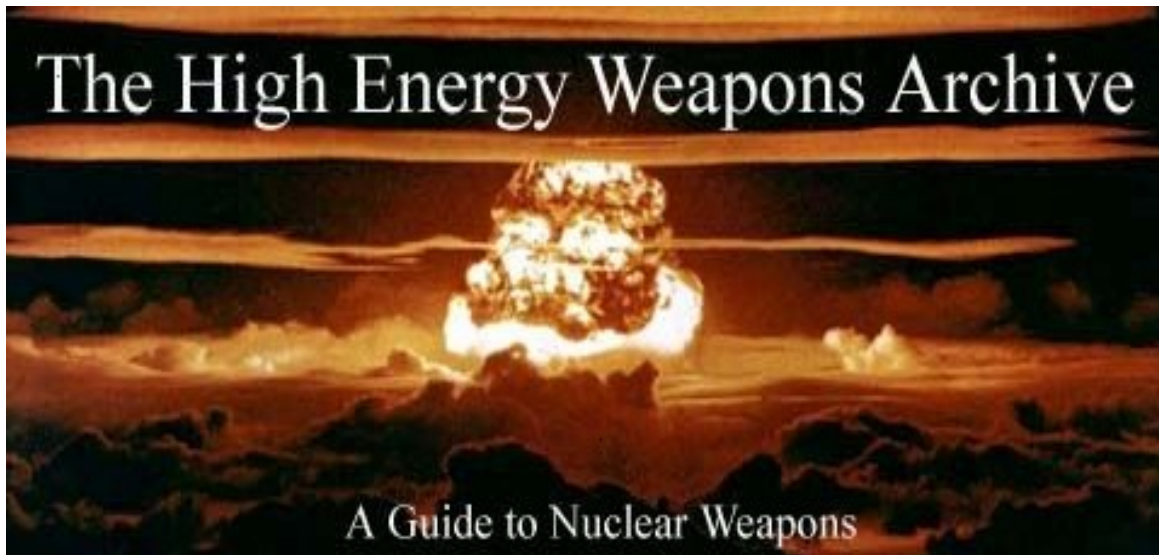
Spreadsheet-type solution of the above equations via an Excel 97 Visual Basic for Application macro may be found using the following Excel 97 Spreadsheets

- Point Mass Ballistic Earth Entry Trajectory – Altitude Integration.xls
- Point Mass Lifting Earth Entry Trajectory – Time Integration.xls

These spreadsheet capabilities provides easy to use numerical input and graphical output in the form of trajectory plots versus altitude based upon fourth-order Runge-Kutta numerical integration of the governing equations of motion. Also output are spherical stagnation point flow properties (assuming thermally perfect, calorically imperfect air) and heat transfer (using the Fay-Riddell correlation). All atmospheric properties (pressure, density, temperature, dynamic pressure, speed of sound, Mach Number, and Reynolds Number) as a function of altitude are determined from the 1976 U.S. Standard Atmospheric model which is included in the macro as an auxiliary subroutine.

Appendix B – Warhead Fact Sheets

The following internet links to warhead fact sheets are taken from the web site



which can be accessed via the home page link

<http://nuketesting.enviroweb.org/hew/>

The purpose of this site is to tell the story of nuclear weapons development and testing through historical documents, photos, and videos and to create an online public domain archive from the large body of U.S. government information about nuclear weapons.

Weapon 62 (The W-62 is the warhead used with the Mk 12 reentry vehicle which arms a portion of the Minuteman III ICBM force. Designed for use on MIRV (multiple independently targeted reentry vehicle) bus upper stage.)

<http://nuketesting.enviroweb.org/hew/Usa/Weapons/W62.html>

Weapon 76 (The W-76 is the warhead used with the Mk 4 reentry vehicle which arms Trident I (C-4) and Trident II (D-5) submarine launched ballistic missiles (SLBMs). Designed for use on MIRV (multiple independently targeted reentry vehicle) bus upper stage.)

<http://nuketesting.enviroweb.org/hew/Usa/Weapons/W76.html>

Weapon 78 (The W-78 is the warhead used with the Mk 12A reentry vehicle which arms a portion of the Minuteman III ICBM force. Designed for use on MIRV (multiple independently targeted reentry vehicle) bus upper stage. The W-78 replaced part of the W-62 to provide an increased hard target kill capability by increasing both accuracy and yield.)

<http://nuketesting.enviroweb.org/hew/Usa/Weapons/W78.html>

Weapon 87 (The W87 warhead belongs to the newest missile warhead family, sharing a design similar to the W88. It was designed for use on the Peacekeeper (MX) ICBM. It combines a relatively high yield with increased accuracy to make it an effective hard target kill weapon. It is hardened against nuclear effects, and has enhanced safety features.)

<http://nuketesting.enviroweb.org/hew/Usa/Weapons/W87.html>

Weapon 88 (The W88 warhead belongs to the newest missile warhead family, sharing a design similar to the W87. It was designed for use on the Trident II (D5) SLBM. It combines a relatively high yield with increased accuracy to make it an effective hard target kill weapon. It is hardened against nuclear effects, and has enhanced safety features.)

<http://nuketesting.enviroweb.org/hew/Usa/Weapons/W88.html>

Soviet Weapons

<http://nuketesting.enviroweb.org/hew/Russia/Sovwarhead.html>